THE ATMOSPHERIC FLUIDIZED-BED COGENERATION AIR HEATER EXPERIMENT

ANL/CP--71464

DE91 010286

W. Podolski, K. Natesan
Argonne National Laboratory

W. Gerritsen, A. Stewart, K. Robinson
Rockwell International

H. Domian
Babcock & Wilcox

W. Roczniak
ABB Combustion Engineering

DISCLAIMER

Paper to be presented at the Eleventh International Conference on FBC, April 21-24, 1991, Montreal, Quebec, Canada.

THE ATMOSPHERIC FLUIDIZED-BED COGENERATION AIR HEATER EXPERIMENT

W. Podolski, K. Natesan
Argonne National Laboratory
Argonne, Illinois

W. Gerritsen, A. Stewart, K. Robinson
Rockwell International
Canoga Park, California

H. Domian
Babcock & Wilcox
Alliance, Ohio

W. Roczniak
ABB/Combustion Engineering
Windsor, Connecticut

ABSTRACT

The U.S. Department of Energy (DOE) sponsored the Atmospheric Fluidized-Bed Cogeneration Air Heater Experiment (ACAHE) to assess the performance of various heat exchanger materials in order to evaluate fluidized-bed combustion (FBC) air heater systems. Westinghouse Electric Corporation and its subcontractors, Babcock & Wilcox, Foster Wheeler Development Corporation, and ABB/Combustion Engineering, specified test conditions and provided test article hardware for the ACAHE. Argonne National Laboratory, through a contract with Rockwell International, conducted tests in the DOE FBC facility located on a Rockwell site in El Segundo, CA. This paper presents an overview of the project, a description of the facility and the test hardware, the test operating conditions, a summary of the operation, and the results of analyzing uncooled materials specimen probes that were exposed in the fluidized bed for various lengths of time.

INTRODUCTION

The U. S. Department of Energy (DOE) sponsored the Atmospheric Fluidized-Bed Cogeneration Air Heater Experiment (ACAHE), which assesses the performance of various heat exchanger materials for fluidized-air heater systems. The ACAHE was carried out by two principal contractors working in parallel: Westinghouse Electric Corporation and Argonne National Laboratory (ANL). Westinghouse and its subcontractors, Babcock & Wilcox (B&W), Foster Wheeler Development Corporation (FW), and ABB/Combustion Engineering (ABB/CE) prepared specifications and hardware for the ACAHE. Through a contract with the Energy Technology and Engineering Center (ETEC) of the Rocketdyne Division of Rockwell International, ANL conducted the tests in the DOE 1.8-m x 1.8 m (6-ft x 6-ft) atmospheric fluidized-bed combustor (AFBC) located on a Rockwell site in El Segundo, CA. The testing at Rockwell was accomplished in 1988 and 1989, and materials performance analysis followed in 1989 and 1990.

A description of air heater cogeneration systems is given in Ref. 1. Before testing at ETEC, ANL prepared an assessment of the information in the literature concerning materials performance under these conditions [2] and conducted bench-scale corrosion studies in simulated FBC environments [3]. This paper presents a brief summary of the testing at ETEC and some results from the examination of uncooled materials specimens exposed for different lengths of time in several locations in the combustor. A comparison of the results of analyses by ANL and the three Westinghouse subcontractors is presented.

AFBC CONFIGURATION

The DOE AFBC test facility (Fig. 1) was designed, built, and operated by Rockwell for research and development of heat exchanger systems and components.

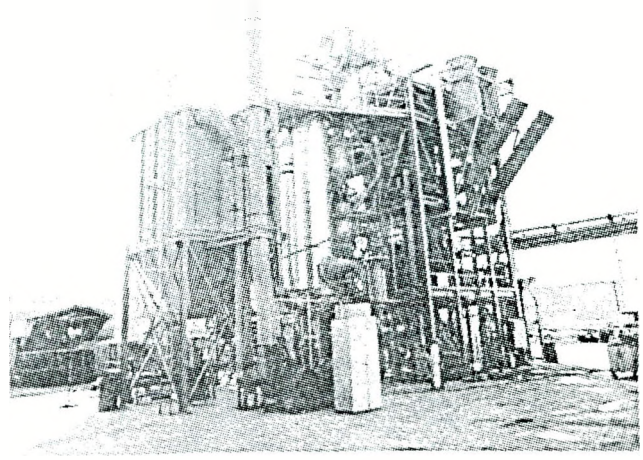

Fig. 1. AFBC Test Facility at Rockwell International in El Segundo, CA

A simplified schematic of the test facility that illustrates the key components is shown in Fig. 2. Air is supplied from the auxiliary compressor and preheater to the top of the combustor tower at 219C (425°F). The air is heated in the convection zone bank, conducted down to the in-bed bank for final heating, and then discharged into the atmosphere at 871°C (1600°F). Tube-material specimens being tested were built into the in-bed tube bundle and were exposed to bed temperatures of 482-871°C (900-1600°F). The bottom row of the in-bed tube bundle was about 0.5 m (~20 in.) above the air distributor.

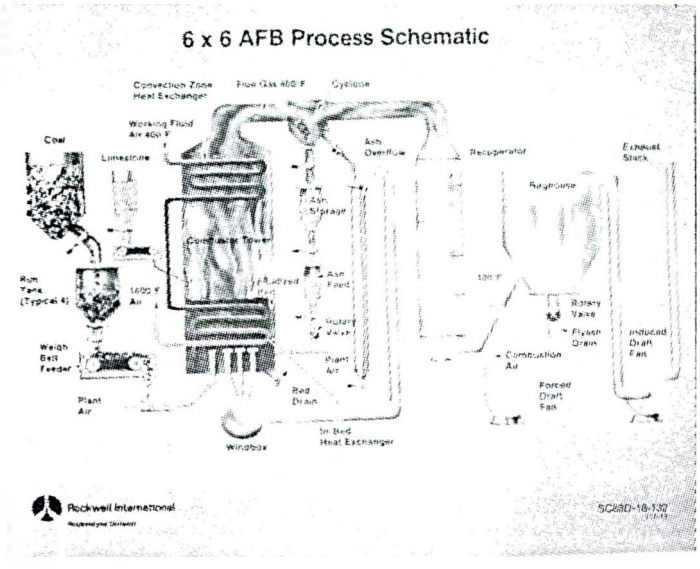

Fig. 2. Schematic Diagram of AFBC Test Facility at Rockwell

Combustion (fluidizing) air, provided by a forced draft fan, passed through a recuperative heat exchanger for preheating before entering the combustor from the bottom through 64 tuyeres. Flue gas leaving the combustor passed through a cyclone separator, a recuperative heat exchanger, a baghouse, and then through an induced draft fan. The cyclone removed most of the larger particulates, which were either collected and recycled into the combustor for improved carbon consumption and limestone utilization or removed from the system for disposal. The baghouse provided final cleanup of the flue gas so that the discharge was cleaner than the new-source air pollution standards for dust emissions.

The coal, limestone, and ash collection-reinjection systems delivered solids into the FBC. Coal was fed independently into each of the four quadrants from run tanks. Limestone was fed into the combustor above the level of the bed, while recycled ash was injected below the bed. Spent bed material, largely calcium sulfate, was manually drained from the bottom of the bed into collection barrels for disposal.

The test facility was manually operated from a nearby control room, which also housed the computerized data acquisition system (DAS). The DAS was programmed to collect data and check alarms without operator intervention. Operators checked the DAS to confirm that the test conditions were within specified limits. Westinghouse team members observed the test operation.

TEST ARTICLE DESCRIPTION

The test articles were selected to provide material wastage information for estimating service life in the erosive/corrosive environment of the fluidized bed. Several types of articles were tested: the platens, the internally cooled specimen probes, the uncooled probes, and a group of tube clamps.

A typical platen is shown in Fig. 3. Of the 24 platens comprising the in-bed tube bundle, 12 were modified to include straight- and bent-tube sections (approximately 110 individual pieces) provided by B&W and FW. These platens contained various types of alloys and some cladded specimens. Some of the platens had expendable thermocouples installed on the exterior surfaces.

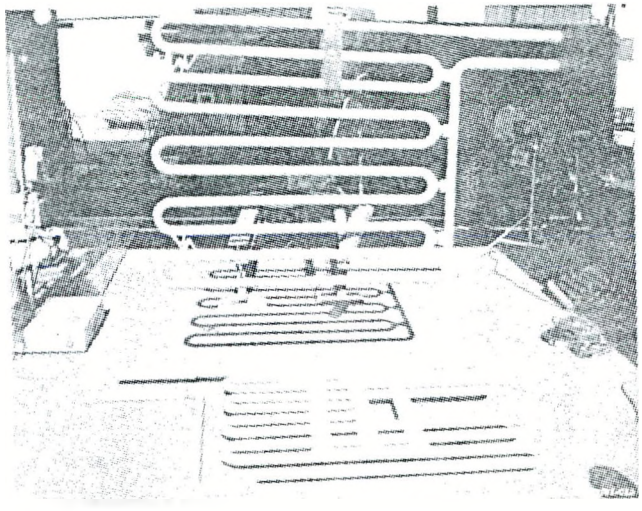

Fig. 3. Typical Platen Used in AFBC Test

Another type of test article was the internally cooled specimen probe (see Fig. 4). There were 14 such probes, each probe having approximately 30 cylindrical specimens. The probes were inserted through the combustor casing at various locations within the fluidized bed, except for one that was above the bed. Each probe was equipped with thermocouples for temperature control. At selected test intervals, the probes were removed and examined.

A third type of test article was a group of uncooled samples of various shapes. The FW and ANL probes used flat or coupon samples that were welded either at an angle (in the FW probe) or flat (in the ANL probe) onto a support rod. The B&W samples were cut sections of rings, which were welded onto the support rod. The ABB/CE samples were ring-shaped. In addition, aluminized and chromized specimens were included in some of the corrosion probes for evaluation. Figure 5 shows a schematic of a B&W specimen probe. Table 1 lists the chemical compositions of various alloys used in uncooled probes of the present test program.

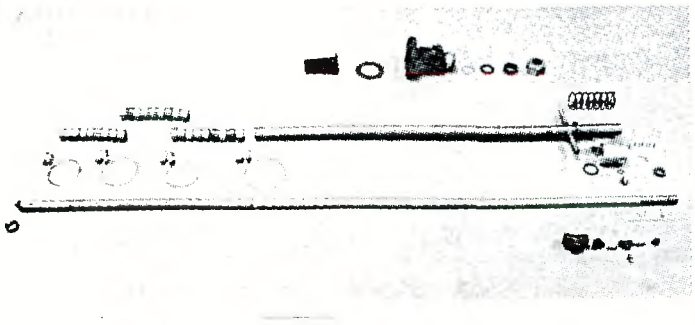

Fig. 4. Internally Cooled Materials Specimen Probe

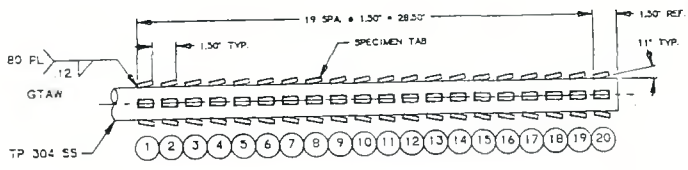

Fig. 5. Materials Probe from Babcock and Wilcox

The remaining test article was a group of 17 tube clamps made from candidate alloys.

TEST OPERATION HIGHLIGHTS

Checkout and shakedown testing of the refurbished facility, with the in-bed specimens installed, was performed in February 1988. Installation of the specimen probes followed the checkout. Table 2 summarizes the test conditions. The combustor was operated for about 1980 h at test conditions. Testing was completed in August 1989.

Data for a number of process parameters were recorded on magnetic tape and transmitted to the project participants. At the completion of the testing, the materials probes were removed, photographed, and sent to their owners for detailed metallurgical evaluation. The tube bundle was also disassembled, and the various platens returned to their suppliers for examination.

OXYGEN PROBE MEASUREMENTS

During the course of testing, the oxygen partial pressure (pO_2) in the combustor was measured with CaO-stabilized ZrO_2 solid electrolyte cells [4].

Table 1. Chemical Composition (wt. %) of Alloys Exposed in Rocketdyne AFBC

Material	C	Cr	Ni	Mn	Si	S	Mo	Al	Fe	Other
304	0.08	18.3	8.10	1.5	0.27	0.018	0.27	-	Bal.[a]	-
800	0.08	20.1	31.7	1.0	0.24	0.006	0.30	0.39	Bal.	Ti 0.31, Cu 0.78
330	0.05	18.6	35.1	1.2	0.92	0.006	0.18	-	Bal.	Nb 0.12
310	0.07	25.0	18.7	1.2	0.64	0.006	-	-	Bal.	-
188	0.08	23.4	23.3	0.7	0.40	-	0.60	0.22	1.40	Co 35.7, W 14.6
556	0.10	22.0	20.0	1.5	0.4	-	3.00	-	Bal	Co 20, W 2.5
253MA	0.10	20.7	10.9	0.3	1.80	-	-	-	Bal.	Ce 0.03
HK40	0.40	28.0	20.0	2.0	2.00	-	0.50	-	Bal.	Cu 0.5
HH	0.32	24.6	11.8	0.4	1.99	0.017	0.19	-	Bal.	-
HP50	0.45	24.3	34.0	0.7	1.73	0.008	0.14	-	Bal.	-
XM19	0.02	21.2	12.5	5.1	0.39	0.004	2.22	-	Bal.	Nb 0.2, V 0.2
Sanicro 33	0.07	22.1	30.3	4.5	0.13	0.003	-	-	-	Nb 0.9, Ce 0.08
8XX	-	20.2	32.5					3	Bal.	
FW 4C	0.05	19.5	20.0	4.9	2.60	-	-	1.40	Bal.	
HR 3C	0.06	24.8	2.0	1.2	0.40	-	-	-		N 0.25 Nb 0.48
347	0.06	18.9	10.8	1.5	0.58	0.014			Bal.	Nb + Ta 057
Ess 1250	0.11	15.4	10.0	6.0	0.59	0.014	0.90		Bal.	Nb 0.26V, 0.94
Temp 30 CrA	0.06	29.2	49.9	0.19	0.29	0.001	1.89		Bal.	Ti 0.17
HR2M	0.02	22.0	14.0	3.0			1.5		Bal.	N2 0.19
HR6W	0.07	22.8	41.9	1.1	0.18	0.002				Nb 0.17, 5.48W, Ti 0.08

[a]Bal. = balance.

Table 2. Steady-State Operating Conditions in AFBC Facility

Parameters	Value	
Fluidized Bed Temperature, average, °C (°F)	871 ± 14	(1600 ± 25)
Fluidized Bed Height, m (in.)	2.41 + 0.15,-0	(95 + 6, -0)
Fluidized Bed Superficial Velocity, m/s (ft/s)	1.52 ± 0.15	(5 ± 0.5)
Flue Gas Oxygen Content, %	4 ± 0.5	
Carbon Consumption, gross, %	98, min[a]	
Working Fluid Outlet Temperature, °C (°F)	816 ± 14	(1500 ± 25)
Working Fluid Inlet Pressure, kPa (psig)	1480	(200, max)
Sulfur Capture, %	90, min	
Coal Type	Illinois #6	
Coal Size, mm (in.)	10	(3/8)
Coal Feed Rate, kg/h (lb/h)	534	(1175)
Limestone Type	Pfizer High Calcium Grit	
Limestone Size, mm (in.)	1.6	(1/16)
Limestone Feed Rate, kg/h (lb/h)	159	(350)
Ca/S, molar ratio	~2.8	

[a]Or best facility capability.

Measurements were made in two ports on the east side of the combustor (locations BMUED and BBTED) and in three ports on the west side of the combustor (locations BTPWC, BMUWC, and BBTWC). Figures 6 and 7

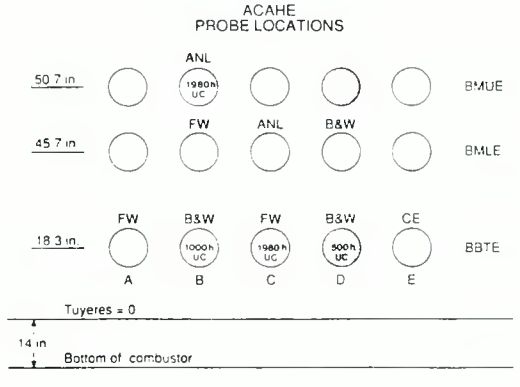

Fig. 6. Oxygen Probe Locations on East Side of Combustor in AFBC

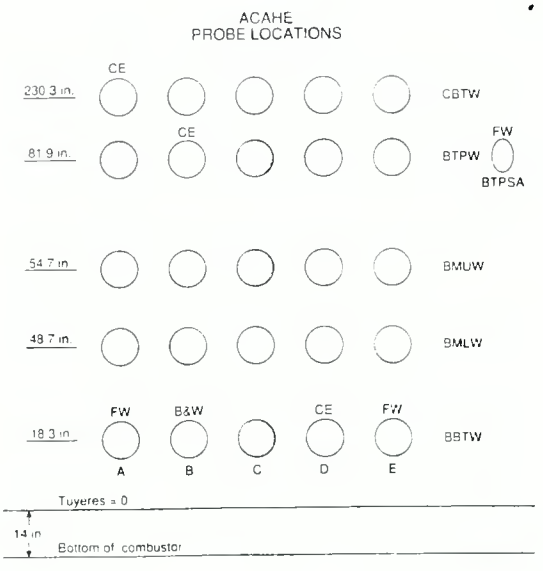

Fig. 7. Oxygen Probe Locations on West Side of Combustor in AFBC

show the locations of the oxygen probes on the east and west sides of the combustor. Also shown in the figures are the locations of the uncooled probes exposed by ANL, B&W, and FW, and ABB/CE, the specimens for which results are reported in this paper.

Extensive corrosion information, developed in laboratory tests under a variety of simulated FBC environments, indicate that high chromium alloys exhibit acceptable corrosion rates when pO_2 in the

environment is 10^{-8} atm or higher [2,5]. The corresponding sulfur partial pressures (pS_2) in such environments will be less than 10^{-20} atm (in the temperature range of 800 to 900°C) and the intergranular penetration of sulfur in the substrate alloy is also minimal. When the pO_2 values fall below 10^{-8} atm, the pS_2 values increase as dictated by the $CaO/CaSO_4$ phase stability line [2,5]. As a result, the oxygen cell measurement data were compiled on the basis of 10^{-8} atm as the value separating oxidation and oxidation/sulfidation regions for the high chromium materials. Figures 8 and 9 show the cell data plotted as a percent of the total time that the local environment had a pO_2 exceeding 10^{-8} atm. The figures show the data obtained from both the east and west walls of the combustor at three different insertion depths, namely, 3 to 12 in., 13 to 24 in., and 25 to 33 inward from the walls of the combustor.

The data in Figs. 8 and 9 show a substantial variation both with exposure time and with distance from the wall. The data indicate that the PO_2 values were above 10^{-8} atm at sensor probe port BMUED for all locations and for exposure period between ~300 and 500 h for only 25 to 50% of the time. Further, the data show that the bed essentially operated under reducing conditions for the second 500 h of exposure of the corrosion probes, the time period of June 16-30, 1988. However, laboratory corrosion test results

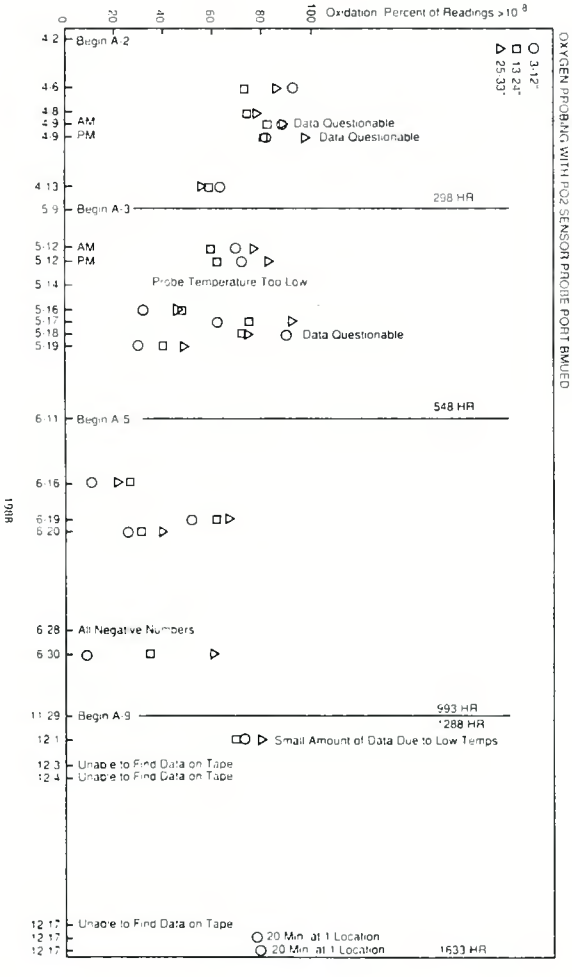

Fig. 8. In-Bed Oxygen Concentration at Port BMUED

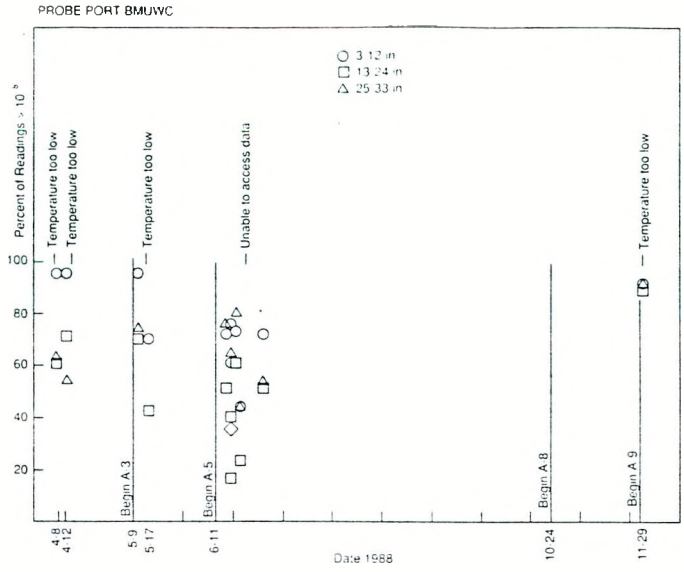

Fig. 9. In-Bed Oxygen Concentration of Port BMUWC

obtained under gas conditions cycling between oxidizing and reducing showed that exposure for as long as 100 h to a sustained low-pO_2 atmosphere is needed to initiate sulfidation attack of high-Cr alloys in SO_2-containing combustion environment[5]. The flue gas sample line developed a leak during the second 500 h of testing, which was interpreted as an insufficient fuel feed rate. During this period, the coal feed rate was increased in order to reduce the flue gas oxygen concentration, which, in effect, decreased the in-bed oxygen concentration, leading to operation under reducing conditions. It can be seen that the oxygen concentrations near the combustor walls were generally lower than in the center of the bed.

CORROSION MECHANISMS

Materials-environment interactions in FBCs indicate that structural alloys develop predominantly oxide scales when exposed at elevated temperatures to O_2-SO_2 gas mixtures of combustion atmospheres [6]. Figure 10 is a schematic of corrosion scale development and morphological changes that occur in Cr_2O_3-forming alloys. The high-Cr alloys develop porous oxide scales (Fig. 10a), and some sulfides are also observed in the inner portions of the scale (in the vicinity of scale/substrate interface). The sulfides are formed by reactions between substrate elements and sulfur that is released when chromium reacts with SO_2 to form external oxide scale. The porosity of the scale enables SO_2 gas molecules to permeate to the scale/substrate interface (Fig. 10b), leading to further oxidation/sulfidation. The released sulfur is transported along the grain boundaries in the metal, leading to internal sulfidation of the alloy (Fig. 10c). Generally, acceptable lifetimes for high-Cr alloys exposed to these environments are determined by the depth of internal sulfidation, which is largely determined by the alloy chemistry, temperature, and SO_2 content of the gas phase. The alumina-forming alloys, in general, are much more

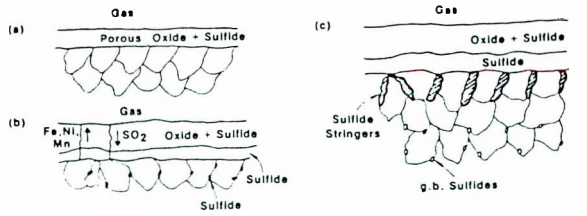

Fig. 10. Schematic of Corrosion Scale Development

resistant to corrosion in these environments, but their scales are susceptible to spallation. When this occurs, the exposed alloy surface is depleted in aluminum; as a result, reformation of protective oxide scale is impeded, and accelerated sulfidation of the base metal ensues.

CORROSION TEST RESULTS

Several uncooled alloy specimens, which were supplied by ANL, B&W, and FW, were analyzed at ANL. Cross sections of specimens were examined using a scanning electron microscope (SEM) equipped with an energy dispersive X-ray analyzer and an electron microprobe to identify the morphological features of corrosion product phases in the scale layers and to establish the thickness of scales and depths of intergranular penetration, if any, of the substrate material.

The specimens exposed in B&W probes were analyzed on both outside and inside surfaces. Since the specimens were welded at an angle to the support rod (see Fig. 5), the inside surfaces were exposed to a deposit of bed material which collected between the specimen and the support rod. The outside surfaces were exposed to moving bed particles in the dynamic bed environment and exhibited very little, if any, deposit material on them. The specimens in the ANL probe were tack welded onto the support rod; (parallel to the rod); consequently, no deposit accumulation was evident during exposure. The specimens in the F&W probe were flat, and the top surface probably acquired bed material deposit.

Figure 11 shows the penetration data for several alloys exposed in B&W probes for 500, 1000, and 1980 h. The data show that the penetration was much less on the outer surfaces of the alloy specimens compared with that on the inside surfaces, which were exposed to deposits of bed material. The penetration on the outer surfaces for all the alloys in Fig. 11 was approximately 100 μm after 1980 h.

The B&W uncooled probe specimens, as analyzed by B&W are summarized in Figure 12. The inside surface penetrations were not analyzed but were found to be very high, in agreement with measurements by ANL. It is seen that, in most cases, the samples exposed for 1980 h in the bed had either less or about the same corrosion as those exposed for 500 and 1500 h. A notable exception was the result for the 8XX alloy which also had much greater corrosion rates than other samples exposed either in the air-cooled probes or in the platen sections. Some of the uncooled specimens which were located above the coal feed ports on probes BBTEB and BBTWB were missing from the probes at the 1000 inspection point. This occurrence and the higher corrosion rates in the samples exposed

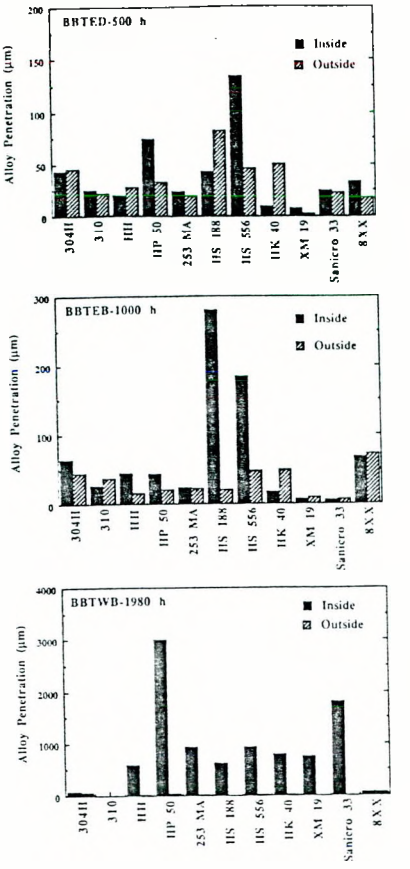

Fig. 11. Corrosion Penetration for Alloys on B&W Probes for (a) 500, (b) 1000, and (c) 1980 h.

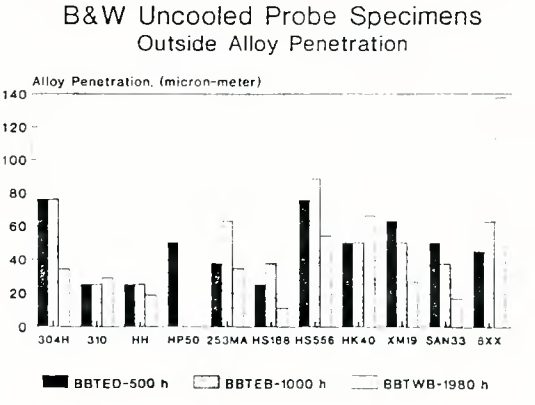

Fig. 12. Penetration Depths on Outside Surface of Alloys Determined by B&W

for 500 h (BBTED) and 1000 h (BBTEB) are thought to be due to the proximity of the probes to the coal feed ports and to local reducing conditions causing greater corrosion than found on probe BBTWB, exposed for 1980 h. These anomolies make it difficult to determine the effect of increased time of exposure for these samples.

On the other hand, the penetration behavior of the different alloys varied based on the penetration on the inside surfaces of the specimens. The data also show the effect of exposure time on the alloy penetration depth, the larger penetration occurring with longer exposure time. Further, the data also indicate susceptibility of some of the alloys, such as HP 50 and Sanicro 33, to internal attack after 1980 h. Most of the other high-Cr alloys (except types 304 and 310 stainless steel and 8XX) exhibited penetrations of 700-1000 μm in 1980 h (60 to 80 mil/yr, based on parabolic kinetics). Figure 13 is a composite plot showing the effect of time on the penetration depths for several alloys exposed in B&W probes. Data for alloys such as HP50 and Sanicro 33 were omitted from this plot.

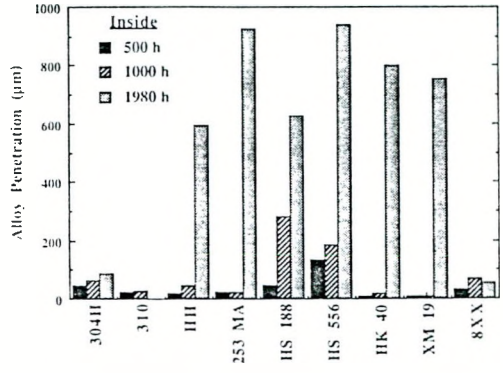

Fig. 13. Corrosion Penetration for Alloys on B&W Probes as a Function of Time

Figure 14 shows similar data for several alloys exposed for 1980 h in the ANL probe BMUEB. The results show that penetration depths were similar on both the inside and outside surfaces of the specimens, indicating that the corrosion behavior in the absence of bed deposit accumulation is nominal and is similar to those reported above for specimens exposed

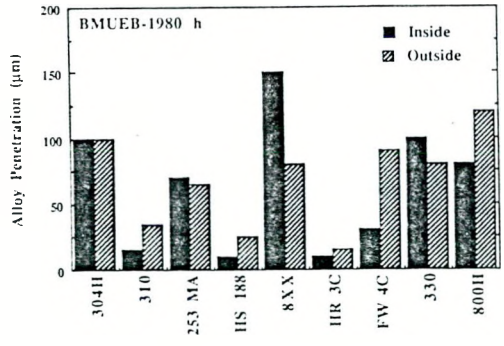

Fig. 14. Corrosion Penetration for Alloys on ANL Probe BMUEB After 1980 h

in B&W probes. Figure 15 shows the penetration depth data for specimens exposed in the FW probe BBTEC for 1980 h. The locations A, B, C, and D in Fig. 15 correspond to 0, 90, 180, and 270° positions along the circumference of the probe; the 0 and 180° locations depict regions exposed to top and bottom of the

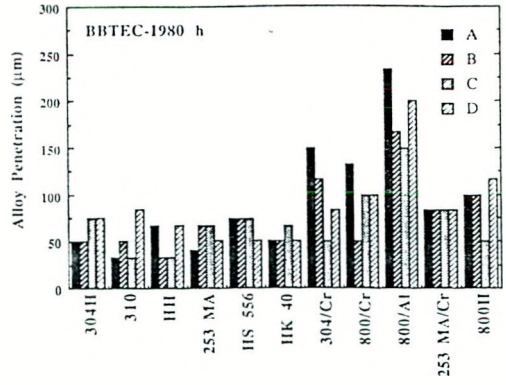

Fig. 15. Comparison Penetration for Alloys on FW Probe BBTEC. (The locations A, B, C, and D Correspond to 90, 180, and 270° Positions Along the Circumference of the Ring.)

bed. Also included in the figure are data for chromized (304/Cr, 800/Cr, and 253 MA/Cr) and aluminized (800/Al) specimens. The results clearly indicate that the alloy penetration rates in this figure are comparable to those presented above for ANL and B&W (outside surface region of samples) probe specimens.

Figure 16 shows a comparison of data from probes exposed (for 1980 h) by the three organizations. The penetration rates for the alloys range between 2 and 20 mil/yr, based on parabolic kinetics.

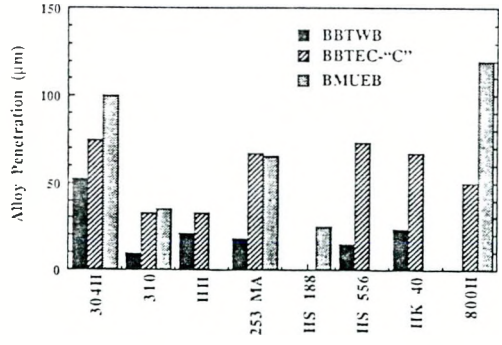

Fig. 16. Comparison of Corrosion Penetration for Outside Surfaces of Alloys on ANL, B&W and FW Probes for 1980 h. (On the BBTEC Probe, the location is at the bottom of the ring.)

Figure 17 shows penetration depth on various alloys as determined by ABB/CE. These results are representative of the behavior seen on the ABB/CE probes and are comparable to the results seen on the ANL, FW and B&W probes.

Figures 18 through 20 show the microstructures of several alloys from ANL probe BMUEB (typical of most of the alloys exposed in different probes) after 1980 h exposure in the AFBC. The top and bottom photographs in the figures correspond to specimens attached to the top and bottom of the support rod.

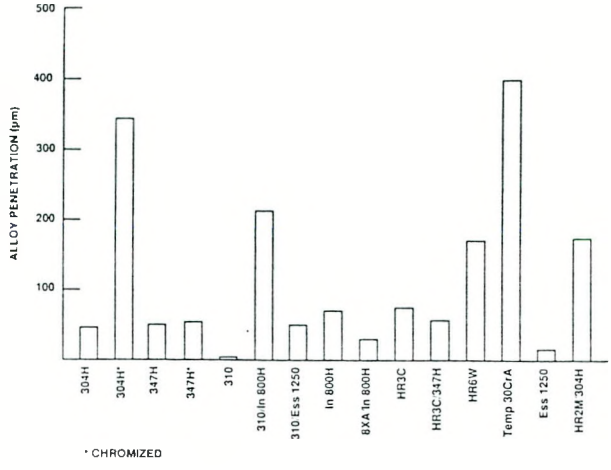

Fig. 17. Penetration Depths on Representative Specimens from ABB/CE Probes.

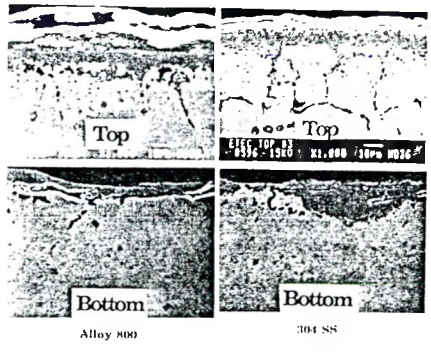

Fig. 18. Microstructures of Alloys 800 and 304SS on ANL Probe BMUEB after 1980 h.

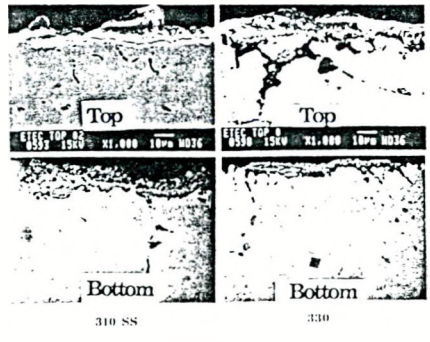

Fig. 19. Microstructures of Alloys 310SS and 330 on ANL Probe MBUEB after 1980 h.

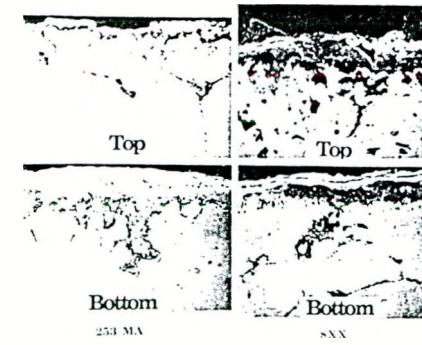

Fig. 20. Microstructures of Alloys 253 MA and 8XX on ANL Probe MBUEB after 1980 h.

In the ANL probe, the specimens were tack welded almost in contact with the support rod and as a result, the inside surfaces were not really exposed to the bed environment. The morphologies of alloy penetration on the outside surfaces of the top and bottom specimens were somewhat different and the extent of penetration was larger in the top specimens. The larger corrosive effect in the top specimens can be attributed to accumulation of the bed deposit material at that location. Detailed analysis of the corrosion products indicated predominantly oxide phases with some isolated sulfide particles in the grain boundary regions of the specimens. None of the specimens exposed in the ANL or FW probes exhibited severe to catastrophic corrosion exhibited by specimens exposed in the B&W probe.

CONCLUSIONS

Materials analysis of cooled probes and platens was completed at the three boiler vendors. These results together with those reported here were used to qualify materials for use in air heater applications. The results are contained in the final project reports (in press) and will be reported elsewhere.

The results obtained from an analysis of the specimens in the uncooled probes indicate that the presence of bed material deposit on the specimen surfaces leads to significant, and sometimes catastrophic, corrosion degradation of materials at a temperature of ~1550°F. On the other hand, the same alloys exhibit acceptable corrosion rates in the range of 2 to 10 mil/y (extrapolated from the 1980 h data based on parabolic kinetics) when the surfaces were devoid of bed material deposits. In this regard, component material surfaces exposed to a corrosive-erosive environment perform superior to those exposed to corrosive environment alone. The acceptable performance of even Alloy 800 (an alloy that has been shown to undergo substantial corrosion in exposures in other FBC facilities) indicate that the combustion atmosphere in the present test was much more benign than the other systems and that the operating conditions/procedures, if duplicated in a commercial system, can result in enhanced reliability of the larger system.

ACKNOWLEDGMENT

This work was performed for the U.S. Department of Energy, Office of Conservation and Renewable Energy, under Contract W-31-109-ENG-38.

REFERENCES

1. Bannister, R. L., Garland, R. V., Carli, G., Datsko, S. C., and Turek, D. G., "Cogeneration with a Fluidized Bed Air Heater, Presented at the 11th International Conference on Fluidized Bed Combustion, Montreal Canada, April 21-24, 1991.

2. Natesan, K., Miller, S. A., and Podolski, W. F., An Assessment of the Performance of Heat Exchanger Materials in Fluidized-Bed Combustors, Argonne National Laboratory Report, ANL-86-42, Nov. 1986.

3. Natesan, K. and Podolski, W. F., Laboratory Tests in Support of Atmospheric Fluidized-Bed Cogeneration Air Heater Experiment: Summary Report, Argonne National Laboratory Report ANL-88-36, July 1988.

4. Campbell, J., "Phase II -Primary Heater Module," Final Report for the Period February 1980 - November 1983, DOE/ETC/15020-1634 (Vol. 2), December 1983, pp. 4-142 - 4-170.

5. Natesan, K., High Temperature Technology, (1986), p. 193.

6. Nateson, K., Laboratory Studies on Corrosion of Materials for Fluidized Bed Combustion Applications, Argonne National Laboratory, ANL/FE-90/1, October 1990.